physics

MDPI

Article

Transverse Dynamics of Strange Hadrons in Relativistic Heavy-Ion Collisions

Diana Deară [1,*], Oana Ristea [1], Cătălin Ristea [2] and Alexandru Jipa [1]

[1] Faculty of Physics, University of Bucharest, 077125 Bucharest-Măgurele, Romania; oana.ristea@gmail.com (O.R.); alexandru.jipa@unibuc.ro (A.J.)
[2] Institute of Space Science—INFLPR (National Institute for Laser, Plasma and Radiation Physics) Subsidiary, 077125 Bucharest-Măgurele, Romania
* Correspondence: dianadeara@yahoo.com

Abstract

We present a study of the mean transverse momentum $\langle p_T \rangle$ of identified strange hadrons ($K^0_S, \Lambda, \overline{\Lambda}, \Xi^-, \overline{\Xi}^+, \phi, \Omega^-, \overline{\Omega}^+$) produced in Au+Au collisions at RHIC-BES energies (the nucleon–nucleon center-of-mass energy $\sqrt{s_{NN}}$ = 7.7 GeV, 11.5 GeV, 19.6 GeV, 27 GeV and 39 GeV). The mean transverse momentum is obtained from transverse momentum spectra of the strange hadrons as measured by the STAR experiment and its dependence on the number of participants N_{part} is studied. For RHIC-BES energies, experimental data indicate a centrality dependence of $\langle p_T \rangle$, with an increase towards central collisions. This dependency is described using a power-law function to fit the data. The power-law exponent α is used to characterize the degree of flattening of $\langle p_T \rangle$ with respect to N_{part} and its dependency on the collision energy and particle mass is studied. Special emphasis is placed on ϕ-meson that has a smaller interaction cross-section, thus reflecting the properties of the early stages of the system's evolution. The $\langle p_T \rangle$ of ϕ-mesons produced in Au+Au collisions at RHIC-BES energies are compared with the results obtained in Au+Au collisions at higher RHIC energies and in Pb+Pb collisions at SPS and LHC energies. A distinct energy dependence of $\phi\langle p_T \rangle$ values is identified. Furthermore, data indicate, when comparing peripheral and central heavy-ion collisions, that ϕ-meson $\langle p_T \rangle$ increases with system size, following two distinct trends. The results are compared with the predictions of the default and string-melting versions of the AMPT generator. We observe that the string-melting AMPT version describes the strange meson $\langle p_T \rangle$, but underpredicts the strange baryon $\langle p_T \rangle$ centrality dependence. The default AMPT overpredicts the K^0_S and ϕ meson $\langle p_T \rangle$ centrality dependence, while the strange baryon data are in general better described by this version of the model. The exponent α obtained from AMPT-simulated results does not describe the measurements satisfactorily.

Keywords: relativistic heavy-ion collisions; strangeness; average transverse momentum; collective flow

Check for updates

Received: 30 September 2025
Revised: 9 April 2026
Accepted: 10 April 2026
Published: 7 May 2026

Copyright: © 2026 by the authors. Licensee MDPI, Basel, Switzerland. This article is an open access article distributed under the terms and conditions of the Creative Commons Attribution (CC BY) license.

1. Introduction

The mapping of the nuclear phase diagram and the study of the behaviour of nuclear matter under extreme conditions of density and temperature remain active areas of research. Relativistic heavy-ion collisions offer the possibility of investigating the nuclear matter under these extreme conditions. The matter produced in these collisions undergoes complex dynamics and can be studied in greater detail through the collective characteristics of the produced systems. In such collisions, a multitude of particles are produced,

whose properties, such as energy and momentum, offer valuable insights into the system's properties and evolution. Among these, strange hadrons serve as highly appropriate probe to investigate the dynamics of high-energy collisions. The enhancement of strange hadrons has been proposed as a signal of quark–gluon plasma (QGP) formation [1,2].

Different regions of the QCD phase diagram can be accessed through nuclear collisions at different energies. The various results from the RHIC-BES energy domain can reveal the change in the behaviour of the system produced in heavy-ion collisions in order to locate the collision energy range where the onset of deconfinement happens. Over the years, strangeness has proven to be an essential tool to study the properties of the matter produced in relativistic nuclear collisions and has revealed a number of intriguing results [3]. In recent years, results from the HADES experiment provide complementary information from heavy-ion collisions at a few GeV [4,5]. STAR experiment data obtained in Au+Au collisions at the nucleon–nucleon center-of-mass energy $\sqrt{s_{\mathrm{NN}}} = 3$ GeV showed that strange particles participate in the collective behaviour of the system and hadronic interactions dominate in the fireball at this energy [6]. The phenomenological parametrizations of strange hadron yields as a function of collision energy and number of participants, along with predictions from different transport models, are given in Ref. [7] for heavy-ion collisions around threshold energies. The present results indicate a beam energy region below 19.6 GeV for further investigation of the deconfinement phase transition [8].

In this paper, the centrality dependence of the mean transverse momentum $\langle p_{\mathrm{T}} \rangle$ of $\mathrm{K}^0_{\mathrm{S}}, \Lambda, \overline{\Lambda}, \Xi^-, \overline{\Xi}^+, \phi, \Omega^-, \overline{\Omega}^+$ produced in Au+Au collisions at RHIC-BES energies is investigated. The data were collected with the STAR experiment, one of the main experiments at RHIC [9,10]. Here, we investigate the behaviour of strange hadrons with respect to the transverse collective flow over a wide energy range (7.7–39 GeV). This phenomenon measured at kinetic freeze-out is crucial in the understanding of the dynamics of a heavy-ion collision because the transverse collective flow is entirely generated in the collision and develops throughout the entire evolution of the system [11,12].

Another possible signal of QGP creation was proposed by Léon Van Hove, suggesting that a plateau-like behaviour in the dependence of $\langle p_{\mathrm{T}} \rangle$ as a function of particle multiplicity may indicate a first-order phase transition from hadronic matter to QGP [13]. It is considered that the particle multiplicity is a measure of the entropy, while $\langle p_{\mathrm{T}} \rangle$ reflects the combined effects of temperature and collective transverse expansion. Therefore, $\langle p_{\mathrm{T}} \rangle$ should increase with the collision energy when the early-stage matter is either in an entirely confined or in an entirely deconfined phase, and it remains approximately constant when the matter is in a mixed phase [13,14]. The energy dependence of the inverse slope parameter of $\mathrm{K}^{\pm}$ produced at midrapidity in Au+Au or Pb+Pb collisions measured at AGS, SPS and RHIC energies has shown a plateau structure in the SPS energy range [14,15]. In this paper, we analyzed the dependence of the mean transverse momentum of strange hadrons produced in Au+Au collisions at $\sqrt{s_{\mathrm{NN}}} = 7.7$–39 GeV on the average number of participating nucleons, N_{part}, based on the earlier results obtained in Au+Au, Cu+Cu and Pb+Pb collisions which showed that the charged particle multiplicity produced in these collisions depends on N_{part} [16–19].

Moreover, to explore how multi-strange hadrons interact within the medium and to enhance our interpretation of the data, the obtained ϕ-meson $\langle p_{\mathrm{T}} \rangle$ results were compared to existing data from RHIC, SPS, and LHC—the latter two accelerators providing the data from Pb+Pb collisions. This comparative approach considers improving the understanding of systems generated in relativistic heavy-ion collisions, offering a more precise view of nuclear matter behaviour under extreme conditions.

https://doi.org/10.3390/physics8020044

2. Study Details

This paper presents a study of the mean transverse momentum $\langle p_T \rangle$ of strange hadrons produced in relativistic nuclear collisions. The mean transverse momentum is obtained from the p_T spectra of produced particles in Au+Au collisions at midrapidity from the Beam Energy Scan (RHIC-BES) programme at RHIC. K^0_S, ϕ, Ω^-, and $\overline{\Omega}^+$ spectra were fitted using an exponential function:

$$\frac{d^2N}{2\pi p_T dp_T dy} = A_e \exp\left(\frac{-(m_T - m_0)}{T}\right), \quad (1)$$

while the Λ, $\overline{\Lambda}$, Ξ^-, and $\overline{\Xi}^+$ spectra were fitted with a Boltzmann function:

$$\frac{d^2N}{2\pi p_T dp_T dy} = A_B m_T \exp\left(\frac{-(m_T - m_0)}{T}\right), \quad (2)$$

where y is the rapidity, $m_T = \sqrt{{m_0}^2 + {p_T}^2}$ is the transverse mass, m_0 is the rest mass of the particle, and $A_e\left(\frac{\text{GeV}}{c}\right)^{-2}$, $A_B\left(\frac{\text{GeV}^{-3}}{c^{-2}}\right)$ and $T(\text{GeV})$ are the fit parameters. The fit range for K^0_S, ϕ, Λ and $\overline{\Lambda}$ was $[0,\ 2]$ GeV/c, and for Ξ^-, $\overline{\Xi}^+$, Ω^- and $\overline{\Omega}^+$ it was $[0,\ 2.6]$ GeV/c at all energies, with c the speed of light.

The mean transverse momentum of the strange particles was obtained by integrating the whole range of p_T spectra as follows [20,21]:

$$\langle p_T \rangle = \frac{\int_0^\infty p_T \left(\frac{dN}{dp_T}\right) dp_T}{\int_0^\infty \left(\frac{dN}{dp_T}\right) dp_T} = \frac{\int_0^\infty p_T dp_T\ p_T \left(\frac{dN}{p_T dp_T}\right)}{\int_0^\infty p_T\ dp_T \left(\frac{dN}{p_T dp_T}\right)} = \frac{\int_0^\infty p_T dp_T\ p_T\ f(p_T)}{\int_0^\infty p_T\ dp_T f(p_T)}, \quad (3)$$

where the functions from Equations (1) and (2) were used to calculate the integrals of $\langle p_T \rangle$.

As the energy increases, the contribution of soft and hard processes in the particle production varies, therefore the study of the particle production dependence with respect both to the number of participant nucleons, N_{part}, and to the number of binary collisions, N_{coll}, is essential. It is considered that particle production scales with N_{part} when there is an intense rescattering phase in the fireball and soft processes dominate. These soft hadrons, which decouple from the collision zone in the late hadronic freeze-out stage of the evolution, can provide information about the fireball dynamics and thermalization degree of the system. Experimental results from SPS confirmed such an N_{part} scaling for the charged particle multiplicity produced in Pb+Pb collisions [16–18]. When relativistic nuclear collisions are modelled as a superposition of binary nucleon–nucleon collisions, hard processes dominate over the soft particle production, and a scaling with N_{coll} is expected. Results from higher RHIC energies and from LHC show that there is quite a large contribution of hard processes to particle production [22–25], while at SPS energies no significant scaling with N_{coll} was observed, indicating that the contribution from hard processes to charged particle production is quite small at this energy range [26].

The HADES experiment K^0_S and Λ yields obtained in Au+Au collisions at $\sqrt{s_{\text{NN}}} = 2.4$ GeV have been parametrized by a power-law dependence on N_{part}, Yield $= a \cdot N_{\text{part}}^{\alpha_Y}$ with a power-law exponent $\alpha_Y = 1.45 \pm 0.06$ [4]. The same behaviour was observed by the STAR Collaboration in Au+Au collisions at $\sqrt{s_{\text{NN}}} = 3$ GeV for K^-, K^0_S and Λ hadron production with similar values within errors of the power-law scaling parameter both for 4π and midrapidity yields [6]. This common scaling of the strange hadrons with N_{part} was interpreted as indicating similar production mechanisms for these particles. As the beam energy increases, at RHIC-BES energies, the α_Y parameter was found to decrease with collision energy and almost to saturate at the RHIC top energy [6]. The

observed behaviour of the power-law exponent α_Y, from values significantly exceeding unity ($\alpha_Y \approx 1.35$–1.45 at HADES and STAR FXT energies to a near-linear dependence ($\alpha \approx 1.1$) at higher RHIC energies, may indicate a change in strangeness production: from hadronic rescatterings in a baryon-stopped medium to partonic production in the hot and dense medium created at higher beam energies.

As the data show that N_{part} dependence is appropriate to describe the strange particle production in heavy-ion collisions at the RHIC-BES energy range, we considered a similar dependence to describe the N_{part} dependence of the mean transverse momentum of these particles. The dependence of $\langle p_T \rangle$ on N_{part} can be parametrized using a power law, analogous to particle yields, since both observables are driven by the same initial-state conditions and reflect the system's response to increasing energy density and pressure gradients with centrality.

Therefore, the $\langle p_T \rangle$ dependence on the collision centrality can be expressed as a function of the number of participant nucleons considering a power-law function as follows [27,28]:

$$\langle p_T \rangle = C \cdot {N_{\text{part}}}^{\alpha}, \tag{4}$$

where C is a normalization coefficient and α is the exponent parameter. While the power-law N_{part} dependence of strange hadron yields reflects the particle production mechanisms, the analogous N_{part} dependence of $\langle p_T \rangle$ is related to the dynamical evolution of the system, providing insights on how the initial compression and subsequent expansion due to the pressure gradients are converted into collective transverse flow. In more central collisions, the increased number of participants leads to a higher energy density within the system, which generates stronger pressure gradients due to the enhanced rescatterings between the fireball constituents. Therefore, a more intense collective flow develops during the system expansion.

Although both particle production mechanisms and system expansion are driven by the collision centrality (N_{part}), the α_Y parameter is sensitive to the inelastic interaction rate, while the α parameter is sensitive to the generated pressure and the collective expansion of the medium.

In the present study, the degree of the flattening of $\langle p_T \rangle$ for strange mesons and baryons produced in Au+Au collisions at $\sqrt{s_{\text{NN}}} = 7.7$–$39$ GeV is characterized with respect to participant number, N_{part}. The α parameter dependence on the particle species and collision energy is studied. A similar study was performed for bulk particles ($\pi^{\pm}$, $K^{\pm}$, p and $\overline{p}$) produced in Au+Au and Pb+Pb collisions in a wide energy range [27,28] showing that such an approach is suitable to describe the N_{part} dependence of the mean transverse momentum.

This study can help to improve the understanding of the particle production of strange particles and their dynamics in this energy domain and can be relevant for the future experiments at FAIR and NICA [29,30].

3. Results

Since the mean transverse momentum of produced particles is obtained by integrating over the particle p_T spectra, it is dominated by the properties of hadronic p_T spectra in the relatively low p_T range. These distributions are essential physical observables in relativistic heavy-ion collision studies and provide information on hot nuclear matter properties such as thermalization and transverse collective flow generated by system expansion in both partonic and hadronic stages. Therefore, it is of interest to analyze $\langle p_T \rangle$ as a function of N_{part} in order to study the system's evolution and correlate with the collective behaviour developed by the produced particles. This approach allows us to see how $\langle p_T \rangle$ varies with the centrality of the collision, taking into consideration each particle species. In more

central collisions, a system that is denser and hotter is formed, leading to stronger radial flow, and thus the $\langle p_T \rangle$ values are expected to be higher than for smaller systems produced in peripheral collisions.

Strange hadrons are considered to be suitable probes to investigate the created medium, as they are not present in the initial state and are produced during the collision. They freeze out earlier than non-strange particles, giving access to early-time dynamics [31].

The dependence of the mean transverse momentum as a function of the number of participants N_{part} is presented for a wide range of beam energies ($\sqrt{s_{\text{NN}}}$ = 7.7 GeV, 11.5 GeV, 19.6 GeV, 27 GeV and 39 GeV). Based on the p_T spectra, the mean transverse momentum was obtained using Equation (3), for all centrality classes provided by the STAR Collaboration data from Refs. [8,32,33].

Figure 1 shows that $\langle p_T \rangle$ increases with N_{part} for all energies, consistent with stronger collective flow in central collisions. This shows a gradual development of the transverse collective motion as the overlapping region increases. In peripheral collisions, a smaller system is created, leading to a weaker collective flow and lower $\langle p_T \rangle$ values. The fireball has a shorter lifetime, and the particles do not have enough time to develop a collective flow that would significantly affect their transverse momentum spectra.

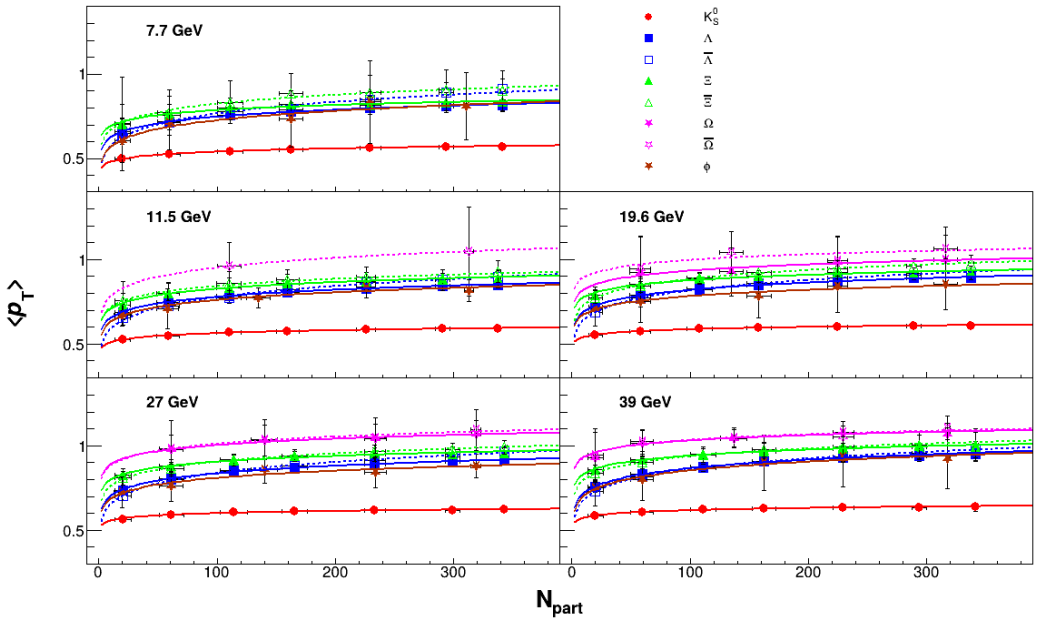


Figure 1. The mean transverse momentum, $\langle p_T \rangle$ as a function of N_{part} for Au+Au collisions at RHIC-BES energy of $\sqrt{s_{\text{NN}}}$ = 7.7–39 GeV. The points are the results obtained using Equation (3), while the lines are the fits for particles and the dashed lines are the fits for antiparticles using a power-law function (4).

Distinct centrality dependence of the mean transverse momentum of strange particles has been observed [34], providing evidence of the influence of the collective flow that is more significant as the interacting region size increases.

It can be observed that $\langle p_T \rangle$ increases with the particle mass for all RHIC-BES energies and all centralities. This is due to the development of the transverse collective flow generated in the hydrodynamic expansion of the fireball. For K^0_S, the increase is less significant than for particles with greater mass. This implies that the contribution of transverse collective flow scales with particle mass; thus, K^0_S hadrons show a weaker centrality dependence [35].

Particles and antiparticles have similar spectral characteristics at midrapidity. Therefore, they possess a similar $\langle p_T \rangle$, within errors, as they interact similarly inside the fireball

and acquire the same collective flow velocity, confirming that the behaviour of identical particles under nuclear forces is charge-independent.

In the RHIC-BES energy range, $\langle p_T \rangle$ values show slight increase as the energy rises.

Figure 2 summarizes the collision energy dependency of the power-law exponent parameter α for the strange hadrons obtained from the power-law fit (4) and presented in Table 1. The α parameter values for K^0_S and ϕ decrease from 7.7 GeV towards 19.6 GeV, while for higher RHIC-BES energies, those values tend to saturate.

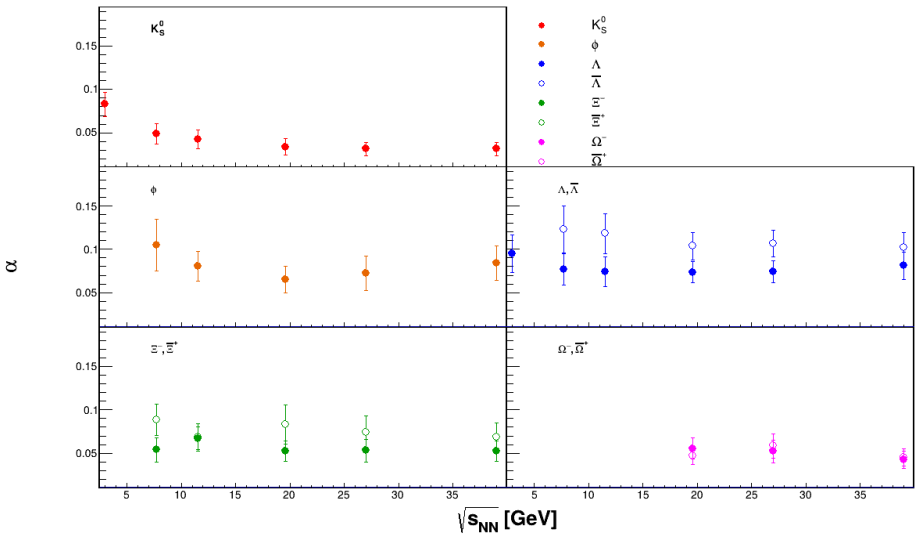


Figure 2. The dependence of the power-law exponent, α, on the collision energy, $\sqrt{s_{NN}}$. The K^0_S and Λ points at $\sqrt{s_{NN}} = 3$ GeV are taken from Ref. [6].

The Λ baryon α values are smaller than those of $\overline{\Lambda}$ baryons over the entire energy range studied. The strongest difference between the two values is for the 7.7–11.5 GeV energy interval. These results can indicate that hadronic processes, such as baryon–antibaryon annihilations due to the baryon-rich environment, influence the final hadron production for the RHIC-BES lower energy region [8]. The energy dependence of various particle ratios showed a maximum at $\sqrt{s_{NN}} \approx 8$ GeV, indicating a maximum net-baryon density around this collision energy [36,37]. Therefore, the annihilation processes have an impact on the slope of p_T spectra for Λ and $\overline{\Lambda}$ baryons, resulting in differences in the N_{part} dependence of $\langle p_T \rangle$ for these baryons. A similar behaviour was observed in Ref. [27] in the case of α parameter values for p and $\overline{p}$ produced in Au+Au collisions at RHIC-BES energies [36], indicating the impact of annihilation processes on antibaryon production due to a higher baryon density in the collision fireball in heavy-ion collisions at lower beam energies.

The K^0_S and Λ data points measured by the STAR experiment in Au+Au collisions at $\sqrt{s_{NN}} = 3$ GeV were included for comparison with the RHIC-BES results. The larger α coefficients at this lower energy suggest that the mean transverse momentum scales more strongly with the number of participants than at higher collision energies, indicating a more efficient transverse expansion driven by the intense pressure of compressed baryonic matter.

For all RHIC-BES energies, a similar difference between $\alpha(\Xi^-)$ and $\alpha(\overline{\Xi}^+,)$ can also be observed; however, this gap between the baryon and antibaryon α values is smaller compared to the Λ-$\overline{\Lambda}$ α comparison. Due to low statistics, the Ω^- and $\overline{\Omega}^+$ p_T spectra at 7.7 GeV are measured for a 0–60% centrality, while for 11.5 GeV, the Ω^- and $\overline{\Omega}^+$ p_T spectra are for a 0–10% and a 10–60% centrality. Therefore, the α parameter for Ω^- and $\overline{\Omega}^+$ was extracted only for the 19.6–39 GeV energy range.

For the higher RHIC-BES energies (19.6–39 GeV), the α parameter values for all strange hadron species, including the Ω^- and $\overline{\Omega}^+$ hadrons, seem to be constant with energy within errors.

Table 1. α and C parameters obtained from the power-law fit function (4). The function uses the $\langle p_T \rangle$ of strange hadrons obtained from p_T spectra and the corresponding number of participants in Au+Au collisions at $\sqrt{s_{NN}} = 7.7$–39 GeV. The resulting χ^2/NDF statistic values are also shown.

Collision Type $\sqrt{s_{NN}}$	Particle Species	C(GeV/c)	α	χ^2/NDF
7.7 GeV	K^0_S	0.430 ± 0.026	0.0491 ± 0.012	0.128/5
	ϕ	0.448 ± 0.123	0.105 ± 0.030	0.088/3
	$\Lambda; \overline{\Lambda}$	0.525 ± 0.050; 0.436 ± 0.0817	0.077 ± 0.018; 0.123 ± 0.027	0.125/5; 0.666/5
	$\Xi^-, \overline{\Xi}^+$	0.612 ± 0.134; 0.548 ± 0.152	0.054 ± 0.014; 0.089 ± 0.018	0.100/5; 0.084/5
11.5 GeV	K^0_S	0.463 ± 0.026	0.042 ± 0.011	0.149/5
	ϕ	0.524 ± 0.115	0.081 ± 0.017	0.259/3
	$\Lambda; \overline{\Lambda}$	0.553 ± 0.049; 0.450 ± 0.053	0.074 ± 0.017; 0.118 ± 0.023	0.067/5; 0.271/5
	$\Xi^-, \overline{\Xi}^+$	0.608 ± 0.099; 0.612 ± 0.132	0.066 ± 0.014; 0.069 ± 0.015	0.097/5; 0.356/5
19.6 GeV	K^0_S	0.501 ± 0.024	0.034± 0.009	0.256/5
	ϕ	0.580 ± 0.164	0.065 ± 0.015	0.048/3
	$\Lambda; \overline{\Lambda}$	0.584 ± 0.037; 0.506 ± 0.041	0.073 ± 0.012; 0.104 ± 0.015	0.378/5; 0.017/5
	$\Xi^-, \overline{\Xi}^+$	0.687 ± 0.071; 0.604 ± 0.069	0.052 ± 0.012; 0.083 ± 0.023	0.395/5; 0.086/5
	$\Omega^-, \overline{\Omega}^+$	0.722 ± 0.153; 0.803 ± 0.180	0.055 ± 0.012; 0.047 ± 0.010	0.036/2; 0.176/2
27 GeV	K^0_S	0.519 ± 0.021	0.031 ± 0.007	0.689/5
	ϕ	0.580 ± 0.143	0.072 ± 0.020	0.214/3
	$\Lambda; \overline{\Lambda}$	0.593 ± 0.038; 0.512 ± 0.040	0.074 ± 0.012; 0.107 ± 0.015	0.102/5; 0.389/5
	$\Xi^-, \overline{\Xi}^+$	0.708 ± 0.067; 0.644 ± 0.063	0.053 ± 0.013; 0.073 ± 0.019	0.160/5; 0.091/5
	$\Omega^-, \overline{\Omega}^+$	0.789 ± 0.154; 0.772 ± 0.144	0.052 ± 0.013; 0.058 ± 0.014	0.021/2; 0.031/2
39 GeV	K^0_S	0.534 ± 0.027	0.031 ± 0.008	0.118/5
	ϕ	0.578 ± 0.094	0.084 ± 0.020	0.042/3
	$\Lambda; \overline{\Lambda}$	0.596 ± 0.047; 0.538 ± 0.046	0.081 ± 0.016; 0.102 ± 0.017	0.113/5; 0.082/5
	$\Xi^-, \overline{\Xi}^+$	0.739 ± 0.101; 0.682 ± 0.084	0.052 ± 0.012; 0.069 ± 0.016	0.034/5; 0.074/5
	$\Omega^-, \overline{\Omega}^+$	0.846 ± 0.190; 0.839 ± 0.188	0.043 ± 0.010; 0.045 ± 0.011	0.138/3; 0.203/3

The mass dependence of the α parameter is presented in Figure 3. The α parameter values for strange hadrons are compared to the values of the α parameter for $\pi^\pm$, $K^\pm$, p and $\overline{p}$ taken from Ref. [27]. For all RHIC-BES energies, the α parameter increases with the particle mass from $\pi^\pm$ to p and $\overline{p}$, and then starts to decrease for ϕ and strange baryons and antibaryons. In a hydrodynamic expansion, the produced particles are moving in the fireball with a common collective flow velocity. The heavier particles ($p/\overline{p}$) receive a larger boost in momentum from this collective flow compared to lighter particles ($\pi^\pm$).

Therefore, in more central collisions, the $\langle p_T \rangle$ of protons grows faster with N_{part} than that of $\pi^{\pm}$, leading to a higher power-law exponent. The decrease in the α parameter for the ϕ-meson and strange baryons may indicate that these particles interact less in the fireball due to their smaller interaction cross-section. Therefore, they acquire less radial flow in the system evolution, leading to a weaker dependence of their $\langle p_T \rangle$ on N_{part}.

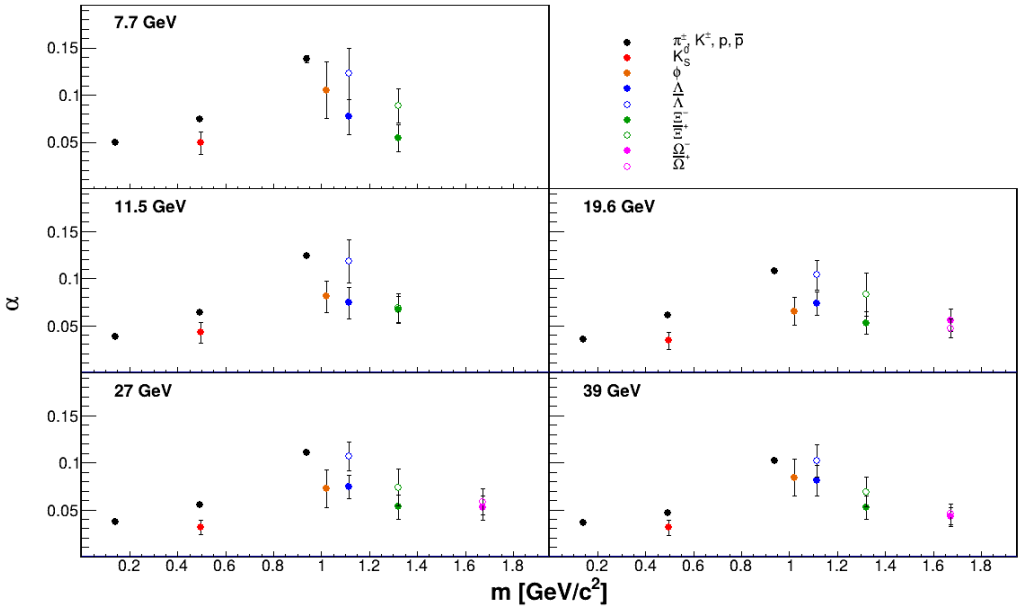


Figure 3. The mass dependence of the power-law exponent, α. The $\pi^{\pm}$, $K^{\pm}$, p and $\overline{p}$ α values (black circles) are taken from Ref. [27].

The degree of flattening in the $\langle p_T \rangle$ dependence on the N_{part} can be related to the α parameter value: a smaller value of the α parameter is correlated to a higher degree of flattening of the distribution, implying a reduced sensitivity of $\langle p_T \rangle$ to centrality. The smallest value for the α parameter among strange hadrons is for $\Omega^- / \overline{\Omega}^+$ hadrons, indicating the largest degree of flattening in the case of these particles.

To compare the results presented in Ref. [27] with the present study, in Figure 4, the parameter α is presented as a function of the number n_s of constituent strange quarks in the studied hadrons. For mesons, the α parameter increases with the number of strange quarks, while for baryons, the α parameter decreases as n_s increases. This behaviour may indicate a competition between mass-dependent hydrodynamics and flavour-dependent decoupling during the fireball's expansion. For mesons, the increase in α from $\pi^{\pm}$ to ϕ-mesons shows that the particle mass is the dominant factor in acquiring radial flow. The higher mass of ϕ compensates for its smaller interaction cross-section to produce a larger radial flow boost than the lighter kaons.

For the baryons (where the mass differences are not so large), the strangeness content becomes significant; as the number of strange quarks increases, the particle reduced hadronic cross-sections lead to a possible sequential freeze-out, causing them to decouple earlier from the fireball and resulting in a decrease in α with n_s.

When comparing the ϕ-meson and p α coefficients, even though the ϕ-meson is heavier than the proton, its smaller α coefficient suggests that its smaller hadronic cross-section causes it to decouple from the system earlier.

A similar behaviour was observed for the mass dependence of the inverse slopes of the transverse mass spectra of particles produced in Pb+Pb collisions at $\sqrt{s_{NN}} = 17$ GeV (the inverse slopes of the Ξ and Ω baryons fall below the linear trend observed for the π, K and p points) [38] and was interpreted as due to an early freeze-out of multi-strange hadrons [39].

Also, the blast-wave (BW) studies for Pb+Pb collisions at SPS energies have shown that strange hadrons decouple from the produced system earlier than the bulk hadrons at a higher freeze-out temperature and have a smaller transverse collective flow velocity [38,40]. A similar BW study, performed on the non-strange and strange particles p_T spectra obtained in Au+Au collisions at RHIC-BES energies, has also shown that the ϕ, Ξ^-, $\overline{\Xi}^+$, Ω^- and $\overline{\Omega}^+$ behaviour in the created fireball is similar, indicating a double kinetic freeze-out scenario due to the separate decoupling of bulk and multi-strange particles [12]. The power-law parameter α behaviour provides support for a double kinetic freeze-out scenario. While the bulk particles remain coupled to the expanding medium through the late-stage hadronic rescattering stage, the ϕ, Ξ and Ω hadrons decouple prematurely. Consequently, their $\langle p_T \rangle$ does not grow as strongly with centrality, and their scaling parameter start to decrease compared to the protons.

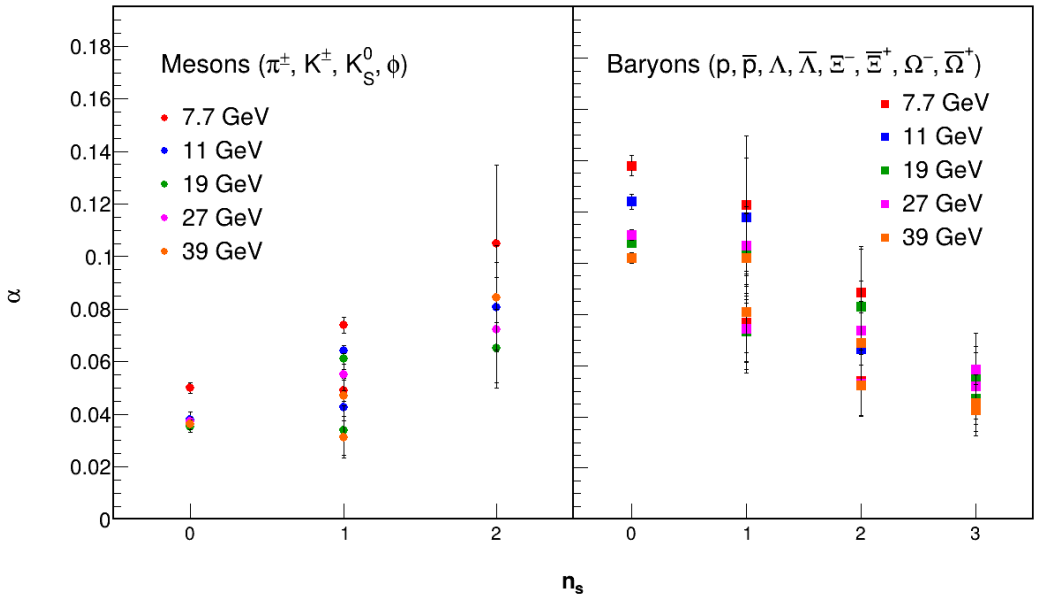


Figure 4. The dependence of the power-law exponent, α, on the number of constituent strange quarks. The $\pi^{\pm}$, $K^{\pm}$, p and $\overline{p}$ α values are taken from Ref. [27].

Multi-strange hadrons such as ϕ-mesons and Ω-hyperons are significant probes of the QGP–hadronic matter phase transition [41,42]. Earlier studies [39,43,44] have suggested that ϕ-mesons have a relatively small hadronic interaction cross-section than ordinary hadrons. Therefore, these particles carry information about the early stages of the system's evolution since they are mostly unaffected by later hadronic rescatterings. However, the nuclear matter produced in heavy-ion collisions at different beam energies and centralities has different size and geometry, as well as various evolution times of possible partonic and hadronic stages.

Figure 5 shows the collision energy dependence of the mean transverse momentum of ϕ-mesons produced at midrapidity ($|y| < 0.5$) in most central Au+Au collisions at $\sqrt{s_{NN}}$ = 7.7–39 GeV Additionally, for comparison, ϕ $\langle p_T \rangle$ measured in central Pb+Pb collisions at $\sqrt{s_{NN}}$ = 6.3–17.3 GeV at SPS [45], in central Au+Au collisions at $\sqrt{s_{NN}}$ = 62.4, 130 and 200 GeV at RHIC [46] and in central Pb+Pb collisions at $\sqrt{s_{NN}}$ = 2.76 and 5.02 TeV [47,48] was added. The SPS results are consistent with the RHIC-BES results from this study. It can be seen that the ϕ $\langle p_T \rangle$ slowly increases with energy from RHIC-BES and SPS energies up to the highest RHIC energy. The LHC data show an increase of about 25% in ϕ $\langle p_T \rangle$ compared to RHIC top energy. The $\langle p_T \rangle$ values are larger for higher energy collisions, indicating increasing radial flow with beam energy.

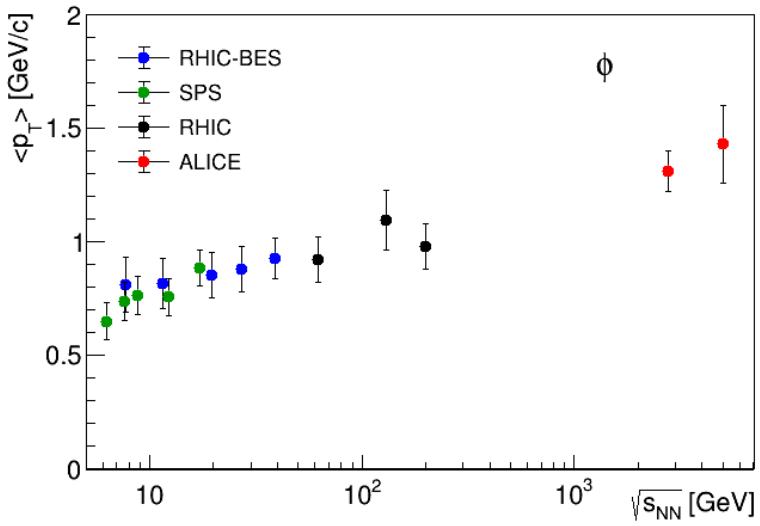


Figure 5. The beam energy dependence of the mean transverse momentum of ϕ-mesons produced in most central Au+Au collisions at RHIC-BES energies (7.7–39 GeV). For comparison, previous results from central Pb+Pb collisions at SPS energies (6.3–17.3 GeV) [45], from central Au+Au collisions at higher RHIC energies (64–200 GeV) [46] and central Pb+Pb collisions at LHC energies (2.76 TeV and 5.02 TeV) [47,48] are also shown.

In Ref. [49], it is considered that $\langle p_T \rangle$ generation has two main sources: the partonic interactions in the early stages of the collision and the fireball expansion in both partonic and hadronic stages. Therefore, the stronger increase from top RHIC energy to LHC energies may point to an interplay between the increased role of partonic degrees of freedom in the fireball and a stronger system expansion and, correspondingly, a significant increased collective radial flow.

The HBT radii scale linearly with the charged pseudorapidity density $(dN_{ch}/d\eta)^{1/3}$ [50,51], and therefore the $(dN_{ch}/d\eta)^{1/3}$ variable can be used as a measure for the system radius in heavy-ion collisions. The system size dependence of the ϕ mesons $\langle p_T \rangle$ produced in central and peripheral Au+Au and Pb+Pb collisions is presented in Figure 6. If one considers that the strength of rescatterings is related to the distance travelled by the produced particles in the system, then $\langle p_T \rangle$ increases with system volume. The data presented in Figure 6 shows two distinct trends: one for central (0–20% centrality for Au+Au collisions at 62.4 GeV, 0–10% centrality for RHIC-BES data, Pb+Pb collisions at 5.02 TeV, and 0–5% centrality for Au+Au collisions at 200 GeV and Pb+Pb collisions at 2.76 TeV) and another for peripheral collisions (60–80% centrality for RHIC-BES data and 60–70% centrality for RHIC and LHC data). The different trend observed in peripheral heavy-ion collisions could be due to the stronger radial pressure gradients created in a shorter lived, smaller volume fireball [52].

Due to its smaller interaction cross-section, the ϕ-meson decouples early and does not follow the full dynamical evolution of the system. At the same time, in central collisions the system size increases strongly with energy. Therefore, the increase in $\langle p_T \rangle$ with system size is slower. In peripheral collisions, the ϕ-mesons also considered to decouple early from the system, but in this case the increase in the system radius with energy is weaker, which leads to a different trend in the behaviour of $\langle p_T \rangle$ with system size. In addition, in peripheral collisions, the uncertainties and systematic effects become essential and may influence the results and trends obtained.

In Ref. [13], the onset of deconfinement is associated with a plateau-like saturation of $\langle p_T \rangle$ as a function of multiplicity, reflecting the change in the nuclear matter equation of state (EoS). Such a plateau-like behaviour was observed for the RHIC-BES energy range in the $\pi^{\pm}$, $K^{\pm}$, p and $\bar{p}$ $\langle m_T \rangle$ mass dependences on the $\sqrt{s_{NN}}$ in Ref. [36]. Since the pions are the most abundant particles in relativistic nuclear collisions due to their low mass, their

rapidity density serves as an indicator of the generated entropy. Therefore, to also consider the π^0 produced in the collision, the pion rapidity density is calculated as

$$\left(\frac{dN}{dy}\right)_{\pi} = 1.5 \cdot \left(\left(\frac{dN}{dy}\right)_{\pi^+} + \left(\frac{dN}{dy}\right)_{\pi^-}\right). \quad (5)$$

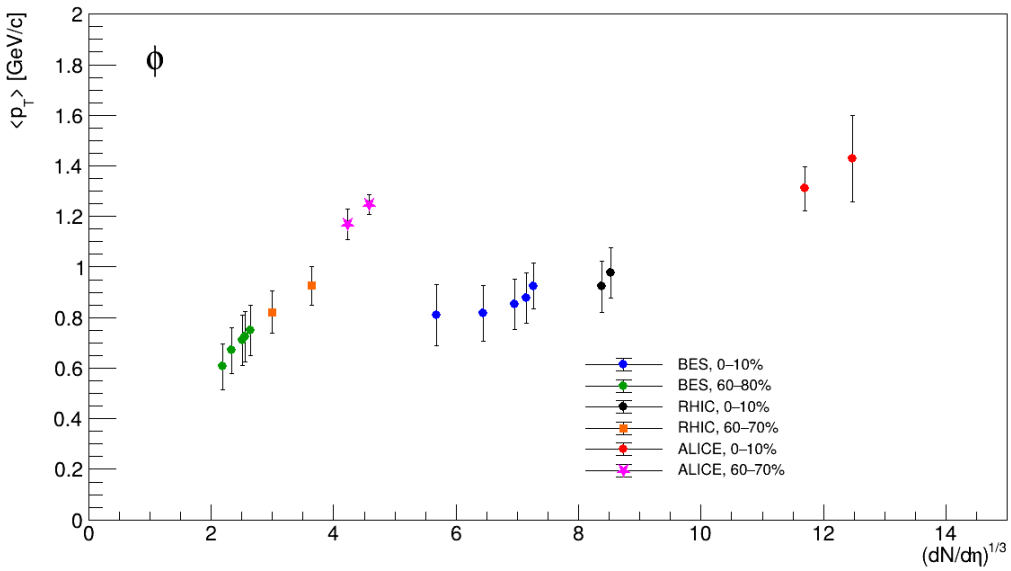


Figure 6. The mean transverse momentum of ϕ mesons produced in central and peripheral heavy-ion collisions as a function of the pseudorapidity density $(dN/d\eta)^{1/3}$ (see text for details). The RHIC and LHC data are taken from Refs. [46–48].

The charged-pion densities were taken from Refs. [36,53,54]. The mean transverse momentum of ϕ-mesons as a function of the π rapidity density is shown in Figure 7. It can be seen that there is a change in the behaviour of mean transverse momentum between the first two lower RHIC-BES energies and 19.6 GeV; after 19.6 GeV, there is a continuous increase with pion rapidity density up to the LHC 2.76 TeV energy. The first two points, corresponding to the 7.7–11.5 GeV energy range, suggest a possible plateau-like behaviour that may indicate the onset of deconfinement at these energies.

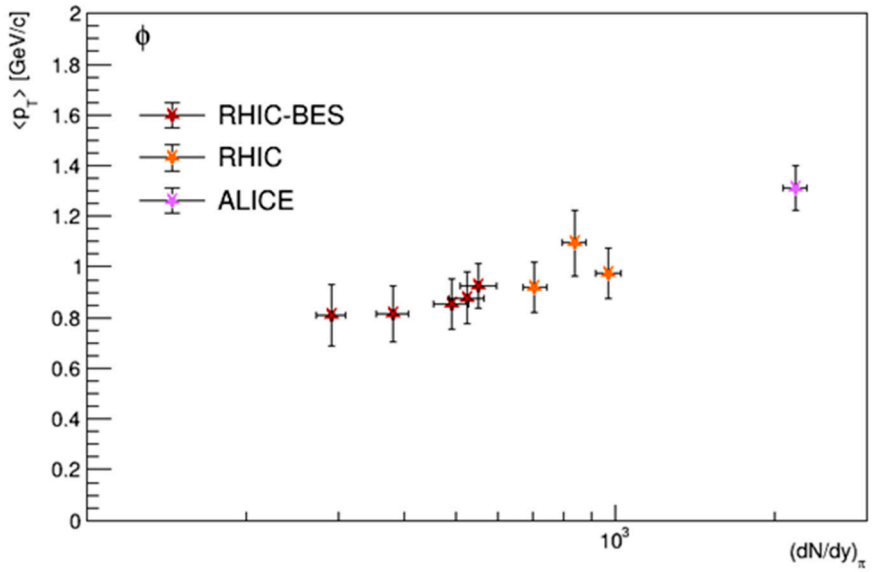


Figure 7. Mean transverse momentum of ϕ-mesons produced in most central heavy-ion collisions as a function of π density. The RHIC and LHC data are taken from Refs. [36,46,47,53,54].

4. Discussion

The dependence of $\langle p_T \rangle$ on the charged-particle multiplicity, N_{ch}, can reveal particle production mechanisms. The increase in $\langle p_T \rangle$ with N_{ch} in pp($\overline{p}$) collisions at various energies [55–57] was explained as due to a hadronization process which contains colour reconnections [58]. The LHC data from pPb collisions cannot be described by a binary collision superposition of pp data, but the collective flow and initial state effects need to be taken into account. In Pb+Pb collisions at LHC energies, a weaker multiplicity dependence is observed and the data are not well enough described by most event generators [59]. At lower beam energies, the particle production is described by a combination of soft and hard processes, with an increased contribution from soft processes as the energy decreases [16,17,26].

In the present study, the participant number dependence of the mean transverse momentum of strange hadrons produced in Au+Au collisions at RHIC-BES energies was studied using a simple power-law function. A similar study performed in Refs. [27,28] for $\pi^{\pm}$, $K^{\pm}$, p and $\overline{p}$ produced in Au+Au and Pb+Pb collisions in a wide energy range showed that the α coefficient is identical for the $\pi^{\pm}$ and $K^{\pm}$ produced in Pb+Pb collisions at $\sqrt{s_{NN}} = 5.02$ TeV, indicating that u, d and s quarks behave the same in the highly thermalized QGP produced in these collisions and there are similar production mechanisms for pions and kaons.

As observed from Table 1 and Figures 2 and 3, the α parameter for strange hadrons shows dependences on both the particle species and collision energy. The α parameter increases with mass for bulk particles ($\pi^{\pm}$, $K^{\pm}$, p and $\overline{p}$) produced in Au+Au collisions at RHIC-BES energies, while for ϕ mesons and strange baryons and antibaryons, it decreases with mass. These results can indicate different shapes in the $\langle p_T \rangle = f(N_{part})$ dependences and, consequently, for p_T spectra. A smaller value of the α parameter indicates a flatter dependence and, consequently, a weaker dependence of $\langle p_T \rangle$ on the participant number. Ξ and Ω baryons, which have smaller hadronic cross-sections, likely decouple earlier, resulting in weaker collective flow and a flatter $\langle p_T \rangle$ dependence [38,40]. Therefore, their mean transverse momentum may exhibit a weaker dependence on the participant number.

The different values of the α parameter for the strange particles and antiparticles are most probably caused by the varying contributions of different mechanisms of production of particles and antiparticles. There is an interplay between particle–antiparticle pair production, which increases with the increasing collision energy and the associated production of strange baryons with kaons through nucleon–nucleon interactions [28]. The yields of the anti-hyperons ($\overline{\Lambda}$, $\overline{\Xi}^{+}$, $\overline{\Omega}^{+}$) and ϕ-meson produced in Au+Au collisions at RHIC-BES increase rapidly with increasing energy [8]. The STAR experiment results have shown that the Ξ and Ω yields increase with energy from 7.7 to 19.6 GeV and then remain almost constant up to energies around 39 GeV. In addition, the absorption of antibaryons due to annihilation in a baryon-rich environment influence the yields and, consequently, the α parameter values.

The α parameter values for strange hadrons decrease with energy for the two lower RHIC-BES energies, while for the 19.6–39 GeV energy range, no energy dependence is obtained. These results are qualitatively consistent with other RHIC-BES observables, which indicate that, at the two lower RHIC-BES energies, the system behaves as a hadron gas, while at higher RHIC-BES energies, deconfined matter can be produced [60–62].

AMPT-generated data were analyzed and compared to experimental data in order to determine how string melting influences particle production and the transverse collective flow observed in nuclear collisions. The AMPT model is a hybrid model for simulating heavy-ion collisions, which includes the initial conditions, partonic interactions, hadronization, and hadronic interactions [63]. There are two versions of the AMPT model: the default

version which focuses on the hadronic interactions and the string-melting (SM) mode which assumes a partonic, deconfined phase and is better suited for heavy-ion collisions where a quark–gluon plasma is expected to form [64].

The initial conditions, describing the spatial and momentum distributions of minijet partons along with string excitations, are generated from the HIJING model [65]. The simulation of parton scatterings and parton transport is performed by Zhang's parton cascade (ZPC) model [66]. In the default version of the AMPT, the minijet partons in the parton cascade recombine with their parent strings to form hadrons via Lund string fragmentation [67], while in the string melting mode, the excited strings are converted to partons and a quark coalescence model is used to describe parton hadronization. Consequently, the evolution of the produced hadrons is governed by a relativistic transport model [68]. For the present study, we used the following parameter values: the QCD coupling constant $\alpha_s = 0.33$ and the screening mass $\mu = 2.265$ fm^{-1}, corresponding to a parton scattering cross-section of $\sigma = 3.0$ mb. The centrality selection was obtained based on impact parameter distribution.

Figure 8 shows the comparison of the K^0_S, Λ, Ξ^-, Ω^- and ϕ experimental results with the AMPT code (default and string-melting versions). The K^0_S and ϕ AMPT-SM results better describe the data for all analyzed energies, while the AMPT-default results are larger compared to the data. In the case of Λ baryons, the AMPT-default results describe better the data within errors, while the SM version underpredicts the data, especially in the 19.6–39 GeV range. For Ξ^- baryons, the lower energies are described better by the SM version, while for the higher RHIC-BES energies, the default version results are closer to the data. For Ω^- baryons, the comparison was made in the 19.6–39 GeV energy range due to incomplete centrality coverage for 7.7 and 11.5 GeV, and it is observed that the default version describes better the $\langle p_T \rangle$ results. These results suggest that there looks to be a change in the underlying strange quark dynamics in the produced matter during Au+Au collisions in the RHIC-BES energy range.

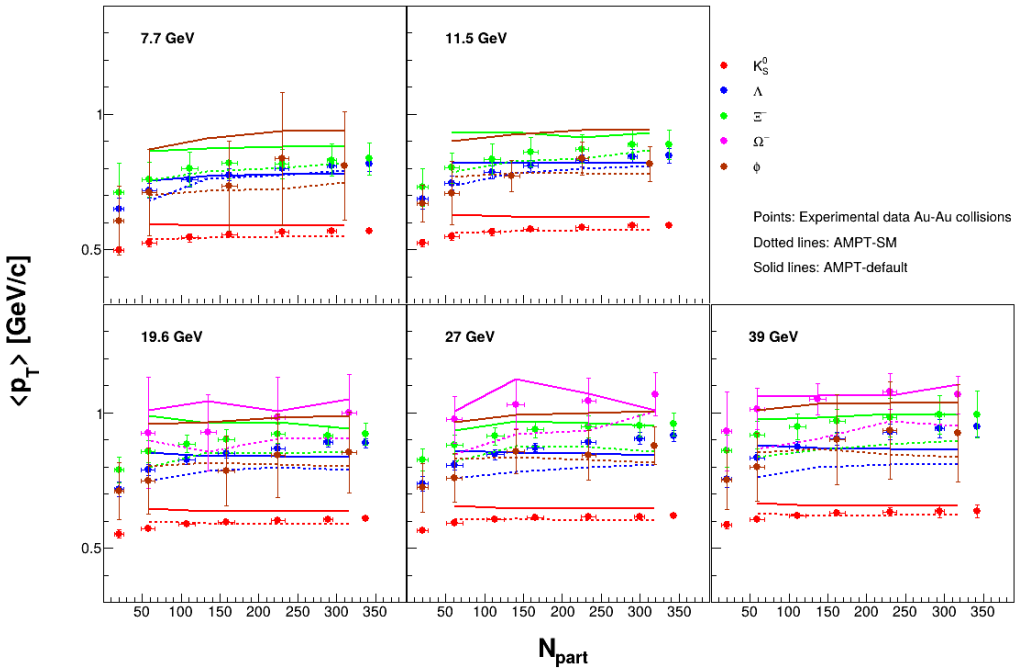


Figure 8. Comparison of the mean transverse momentum of strange hadrons produced in Au+Au collisions as a function of N_{part} with the predictions of the two versions of the AMPT code (see text for details).

The centrality dependence of the simulated mean transverse momentum was studied using Equation (4), and the extracted α parameter values are presented in Figure 9. For K^0_S, Λ, Ξ^-, and Ω^-, the AMPT-SM α values are larger than the default version AMPT α values; however, both AMPT model versions underestimate the α parameter values obtained based on the experimental data. In Figure 8, a weaker centrality dependence of the mean transverse momentum is observed in the simulated data, which determines much smaller values of the α parameter. Therefore, we observe that neither the default nor the SM model found to consistently describe the energy dependence of the α parameter.

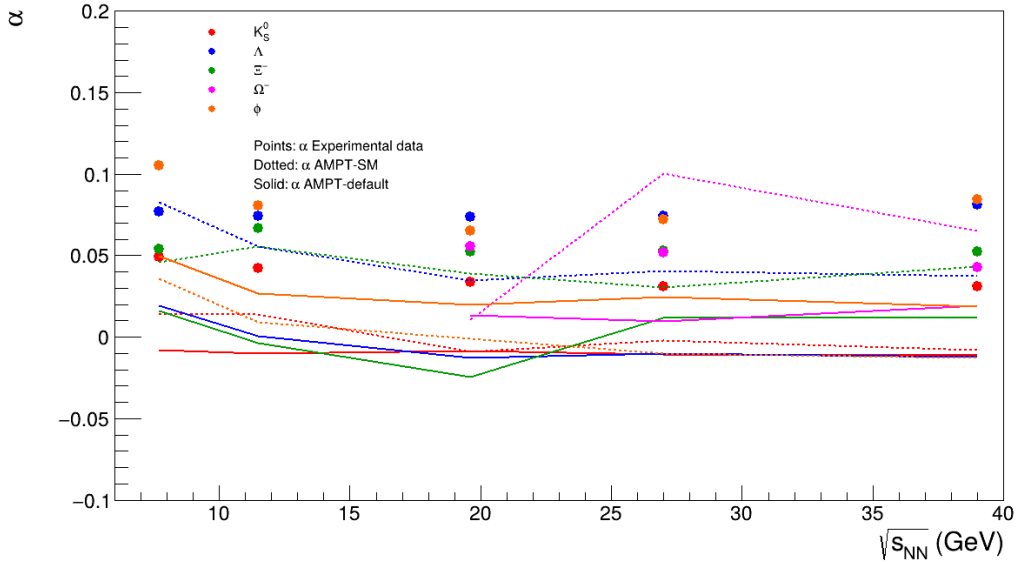


Figure 9. Comparison of the power-law α parameter values obtained using the default AMPT and SM versions.

5. Conclusions

In summary, the study of the mean transverse momentum of particles produced in relativistic nuclear collisions provides insights into the properties and dynamics of the system created.

The mean transverse momentum of strange hadrons produced in Au+Au collisions at RHIC-BES energies $\sqrt{s_{NN}} = 7.7$ GeV, 11.5 GeV, 19.6 GeV, 27 GeV, and 39 GeV, as a function of N_{part} was presented.

In the studied Au+Au collisions, for each strange particle species, the results showed that the mean transverse momentum values are higher in central collisions than in peripheral ones, suggesting a gradual development of the radial flow with increasing system volume.

Additionally, the mean transverse momentum, $\langle p_T \rangle$, increases with increasing mass of the particles for all energies considered in this study. This supports the interpretation that the increase in transverse momentum scales with particle mass, due to the influence of the collective flow. Particles with a smaller mass are less influenced by this flow compared to particles with a larger mass. A slight increase in mean transverse momentum with increased energy in the RHIC-BES energy range was observed.

In this study, the energy dependence on the power-law exponent parameter α of strange hadrons indicates that for the two mesons considered in this study, K^0_S and ϕ, α decreases from 7.7 GeV towards 19.6 GeV, after which the values remain approximately constant for higher energies. Moreover, for the two lower RHIC-BES energies, the α values are smaller for Λ and Ξ^- baryons compared to their corresponding antiparticle values.

This discrepancy is less significant for Ξ^- and $\overline{\Xi}^+$ baryons. Starting from 19.6 GeV, the α values for all particles considered show a weaker energy dependence.

For each energy considered, the α parameter as a function of particle mass was shown. Alongside the strange hadrons considered throughout this study, this analysis included $\pi^{\pm}$, $K^{\pm}$, p and $\overline{p}$. The α parameter values are linked to the degree of flattening of $\langle p_T \rangle$. Smaller α values indicate a weaker dependence of $\langle p_T \rangle$ on N_{part}. It was observed that the α parameter shows an increasing trend with particle mass from $\pi^{\pm}$ up to the p and $\overline{p}$ mass, beyond which, for heavier particles, it starts to decrease.

The energy dependence of the $\langle p_T \rangle$ of ϕ-meson was studied over a wide range of energy (using data from RHIC-BES, RHIC, SPS and LHC). $\langle p_T \rangle$ increases gradually with energy, while a more significant increase is seen in the LHC data compared to the highest RHIC energy. The centrality and system size dependence of $\phi\langle p_T \rangle$ was shown. Two distinct trends were observed: one for central collisions, where the system radius grows rapidly with energy, but the increase in $\langle p_T \rangle$ remains slow due to the early decoupling of ϕ-meson, and another for peripheral collisions, where a smaller, shorter-lived fireball is formed, leading to a steeper increase in $\langle p_T \rangle$ values. These two distinct trends highlight the influence of the system size and medium lifetime on the development of collective flow which contributes to the $\langle p_T \rangle$ values.

The dependence of $\langle p_T \rangle$ of ϕ-mesons on the π rapidity density, considered as a measure of the produced entropy, showed a possible plateau-like shape in the 7.7–11.5 GeV energy range, which can suggest the appearance of a mixed phase during a first-order QCD phase transition at these energies.

The comparison between the experimental data and the AMPT model calculations showed that $\langle p_T \rangle$, of strange mesons is better described by the AMPT string-melting version, while this version underestimates the strange baryons $\langle p_T \rangle$. The AMPT default version provides a better overall description of the strange baryon $\langle p_T \rangle$, but it overestimates the centrality dependence of K^0_S and ϕ-mesons. Furthermore, it was observed that the α parameter obtained from AMPT generated data fails to reproduce the energy dependence of the power-law exponent α observed in the experimental results.

Author Contributions: Conceptualization, D.D. and O.R.; data curation, D.D. and O.R.; formal analysis, D.D.; funding acquisition, A.J.; investigation, D.D. and O.R.; methodology, O.R. and C.R.; software, C.R.; supervision, O.R. and A.J.; validation, O.R. and A.J.; visualization, D.D.; writing—original draft, D.D. and O.R.; writing—review and editing, O.R. and A.J. All authors have read and agreed to the published version of the manuscript.

Funding: This work was supported by Romanian Ministry of Research, Innovation and Digitalization through Institute of Atomic Physics (IFA) coordinating agency, FAIR-RO programme, under contract FAIR-RO/RD/2024_002/ 08.07.2024.

Data Availability Statement: The data presented in this study are available upon request from the corresponding author.

Conflicts of Interest: The authors declare no conflicts of interest.

Abbreviations

The following abbreviations are used in this manuscript:

AGS	Alternating Gradient Synchrotron
ALICE	A Large Ion Collider Experiment
AMPT	A Multi-Phase Transport Model
BES	Beam Energy Scan
BW	blast wave

ch	charged
coll	collisions
EoS	equation-of-state
FAIR	Facility for Antiproton and Ion Research
FXT	FiXed-Target
HADES	High Acceptance Di-Electron Spectromete
HBT	Hanbury Brown and Twiss (effect)
HIJING	Heavy Ion Jet INteraction Generator
LHC	Large Hadron Collider
NDF	number of degrees of freedom
NICA	Nuclotron-based Ion Collider fAcility
NN	nucleon-nucleon
part	participants
QCD	quantum chromodynamics
QGP	quark-gluon plasma
RHIC	Relativistic Heavy Ion Collider
SM	string-melting
SPS	Super Proton Synchrotron
STAR	Solenoidal Tracker at RHIC
T	transverse
ZPC	Zhang's parton cascade

References

1. Feng, Y.-T.; Song, Z.-Y.; Shao, F.-L.; Song, J. Collision centrality and energy dependence of strange hadron production in Au+Au collisions at $\sqrt{s_{NN}}$ = 7.7–54.4 GeV. *Phys. Rev. C* **2023**, *107*, 024909. [CrossRef]
2. Adam, J. et al. [ALICE Collaboration]. Enhanced production of multi-strange hadrons in high-multiplicity proton-proton collisions. *Nat. Phys.* **2017**, *13*, 535–539. [CrossRef]
3. Blume, C.; Markert, C. Strange hadron production in heavy ion collisions from SPS to RHIC. *Prog. Part. Nucl. Phys.* **2011**, *66*, 834–879. [CrossRef]
4. Adamczewski-Musch, J. et al. [HADES Collaboration]. Sub-threshold production of K^0_S mesons and Λ hyperons in Au+Au collisions at $\sqrt{s_{NN}}$ = 2.4 GeV. *Phys. Lett. B* **2019**, *793*, 457–463. [CrossRef]
5. Spies, S. (for the HADES Collaboration). Recent results from Ag+Ag collisions at $\sqrt{s_{NN}}$ = 2.55 GeV measured by HADES. *EPJ Web Conf.* **2022**, *259*, 01007. [CrossRef]
6. Abdulhamid, M.I. et al. [The STAR Collaboration]. Strangeness production in $\sqrt{s_{NN}}$ = 3 GeV Au+Au collisions at RHIC. *J. High Energy Phys.* **2024**, *2024*, 139. [CrossRef]
7. Piasecki, K.; Piotrowski, P. Systematics of yields of strange hadrons from heavy-ion collisions around threshold energies. *Eur. Phys. J. A* **2023**, *59*, 272. [CrossRef]
8. Adam, J. et al. [STAR Collaboration]. Strange hadron production in Au+Au collisions at $\sqrt{s_{NN}}$ = 7.7, 11.5, 19.6, 27, and 39 GeV. *Phys. Rev. C* **2020**, *102*, 034909. [CrossRef]
9. Bhalerao, R.S. Relativistic heavy-ion collisions. In *2012 Asia–Europe–Pacific School of High-Energy Physics. Proceedings*; Kawagoe, K., Mulders, M., Eds.; CERN: Geneva, Switzerland, 2014; pp. 219–240. [CrossRef]
10. Relativistic Heavy Ion Collider. The STAR Detector. Available online: https://www.bnl.gov/rhic/star.php (accessed on 9 April 2026).
11. Ristea, O.; Ristea, C.; Jipa, A.; Calin, M.; Esanu, T. Study of strange particle p_T spectra in heavy-ion collisions at relativistic energies. *EPJ Web Conf.* **2023**, *290*, 05003. [CrossRef]
12. Ristea, O.; Ristea, C.; Jipa, A. Study of strange particle p_T spectra in relativistic heavy-ion collisions with blast-wave model. *Int. J. Mod. Phys. E* **2022**, *31*, 2250090. [CrossRef]
13. Van Hove, L. Multiplicity dependence of p_t spectrum as a possible signal for a phase transition in hadronic collisions. *Phys. Lett. B* **1982**, *118*, 138–140. [CrossRef]
14. Gorenstein, M.I.; Gaździcki, M.; Bugaev, K.A. Transverse activity of kaons and deconfinement phase transition in nucleus–nucleus collisions. *Phys. Lett. B* **2003**, *567*, 175–178. [CrossRef]
15. Gorenstein, M.I. Signals of deconfinement transition in nucleus—nucleus collisions. In *Structure and Dynamics of Elementary Matter*; Greiner, W., Itkis, M.G., Reinhardt, J., Güçlü, M.C., Eds.; Springer Science+Business Media, B.V.: Dordrecht, The Netherlands, 2004; pp. 265–276. [CrossRef]

16. Aggarwal, M.M. et al. [The WA98 Collaboration]. Scaling of particle and transverse energy production in ^{208}Pb+^{208}Pb collisions at 158 *A* GeV. *Eur. Phys. J. C* **2001**, *18*, 651–663. [CrossRef]
17. Antinori, F. et al. [The WA97and NA57 Collaborations]. Determination of the number of wounded nucleons in Pb+Pb collisions at 158 A GeV. *Eur. Phys. J. C* **2000**, *18*, 57–63. [CrossRef]
18. Siklér, F. (for the NA49 Collaboration). Hadron production in nuclear collisions from the NA49 experiment at 158 GeV/c·A. *Nucl. Phys. A* **1999**, *661*, 45–54. [CrossRef]
19. Kumar, A.; Srivastava, P.K.; Singh, B.K.; Singh, C.P. Charged hadron multiplicity distribution at Relativistic Heavy-Ion Colliders. *Adv. High Energy Phys.* **2013**, *2013*, 352180. [CrossRef]
20. Sahoo, R. Relativistic kinematics. *arXiv* **2016**, arXiv:1604.02651. [CrossRef]
21. Sahoo, R. *Relativistic Kinematics. A Journey in Spacetime*; Springer Nature Switzerland AG: Cham, Switzerland, 2025. [CrossRef]
22. Back, B.B. et al. [PHOBOS Collaboration]. Charged-particle multiplicity near midrapidity in central Au+Au collisions at $\sqrt{s_{NN}}$ = 56 and 130 GeV. *Phys. Rev. Lett.* **2000**, *85*, 3100–3104. [CrossRef]
23. Adcox, K. et al. [PHENIX Collaboration]. Centrality dependence of charged particle multiplicity in Au–Au collisions at $\sqrt{s_{\mathrm{NN}}}$ = 130 GeV. *Phys. Rev. Lett.* **2001**, *86*, 3500–3505. [CrossRef]
24. Bearden, I.G. et al. [BRAHMS Collaboration]. Charged particle densities from Au+Au collisions at $\sqrt{s_{\mathrm{NN}}}$ = 130 GeV. *Phys. Lett. B* **2001**, *523*, 227–233. [CrossRef]
25. ALICE Collaboration. Centrality dependence of charged-particle pseudorapidity density at midrapidity in Pb–Pb collisions at $\sqrt{s_{\mathrm{NN}}}$ = 5.36 TeV. *arXiv* **2025**, arXiv:2504.02505. [CrossRef]
26. Abreu, M.C. et al. [NA50 Collaboration]. Scaling of charged particle multiplicity in Pb–Pb collisions at SPS energies. *Phys. Lett. B* **2002**, *530*, 43–55. [CrossRef]
27. Olimov, K.K.; Lebedev, I.A.; Tukhtaev, B.J.; Fedosimova, A.I.; Liu, F.-H.; Khudoyberdieva, S.A.; Kanokova, S.Z. Evolution of midrapidity average transverse momentum of pions, kaons, protons and antiprotons in Au+Au collisions in $(s_{nn})^{1/2}$ = 7–39-GeV energy range from the beam energy scan program. *Int. J. Mod. Phys. E* **2023**, *32*, 2350066. [CrossRef]
28. Olimov, K.K.; Liu, F.-H.; Musaev, K.A.; Olimov, A.K.; Tukhtaev, B.J.; Saidkhanov, N.S.; Yuldashev, B.S.; Olimov, K.; Gulamov, K.G. Particle species and collision energy dependencies of the midrapidity average transverse momenta of identified charged particles in Au+Au and Pb+Pb in $(s_{nn})^{1/2}$ = 62–5020 GeV energy range at RHIC and LHC. *Int. J. Mod. Phys. E* **2021**, *30*, 2150029. [CrossRef]
29. Ablyazimov, T.; Abuhoza, A.; Adak, R.P.; Adamczyk, M.; Agarwal, K.; Aggarwal, M.M.; Ahammed, Z.; Ahmad, F.; Ahmad, N.; Ahmad, S.; et al. Challenges in QCD matter physics—The scientific programme of the Compressed Baryonic Matter experiment at FAIR. *Eur. Phys. J. A* **2017**, *53*, 60. [CrossRef]
30. Geraksiev, N.S. et al. [NICA/MPD Collaboration]. The Nuclotron-based Ion Collider Facility Project. The physics programme for the Multi-Purpose Detector. *J. Phys. Conf. Ser.* **2019**, *1390*, 012121. [CrossRef]
31. Zhou, Y. (for the STAR Collaboration). Strange hadron production in Au+Au collisions at RHIC Beam Energy Scan. *EPJ Web Conf.* **2023**, *276*, 03006. [CrossRef]
32. Ackermann, K.H. et al. [STAR Collaboration]. STAR detector overview. *Nucl. Instrum. Meth. Phys. Res. A Accel. Spectrom. Detect. Assoc. Equip.* **2003**, *499*, 624–632. [CrossRef]
33. Adamczyk, L. et al. [STAR Collaboration]. Probing parton dynamics of QCD matter with Ω and ϕ production. *Phys. Rev. C* **2016**, *93*, 21903. [CrossRef]
34. The STAR Collaboration. Strangeness production in $\sqrt{s_{\mathrm{NN}}}$ = 3 GeV Au+Au collisions at RHIC. *arXiv* **2024**, arXiv:2407.10110. [CrossRef]
35. Abdallah, M.S. et al. [STAR Collaboration]. K^{*0} production in Au+Au collisions at $\sqrt{s_{NN}}$ = 7.7, 11.5, 19.6, 27, and 39 GeV from RHIC beam energy scan. *Phys. Rev. C* **2023**, *107*, 034907. [CrossRef]
36. Adamczyk, L. et al. [STAR Collaboration]. Bulk properties of the medium produced in relativistic heavy-ion collisions from the beam energy scan program. *Phys. Rev. C* **2017**, *96*, 044904. [CrossRef]
37. Randrup, J.; Cleymans, J. Exploring high-density baryonic matter: Maximum freeze-out density. *Eur. Phys. J. A* **2016**, *52*, 218. [CrossRef]
38. Antinori, F. et al. [The NA57 Collaboration]. Study of the transverse mass spectra of strange particles in Pb–Pb collisions at 158 *A* GeV/c. *J. Phys. G* **2004**, *30*, 823–840. [CrossRef]
39. Abelev, B.I. et al. [STAR Collaboration]. Partonic flow and ϕ-meson production in Au+Au collisions at $\sqrt{s_{NN}}$ = 200 GeV. *Phys. Rev. Lett.* **2007**, *99*, 112301. [CrossRef] [PubMed]
40. Bruno, G.E. (for the NA57 Collaboration). Blast-wave analysis of strange particle m_{T} spectra in Pb–Pb collisions at the SPS. *J. Phys. G* **2005**, *31*, S127–S134. [CrossRef]
41. Mohanty, B.; Xu, N. Probe of the QCD phase diagram with ϕ-mesons in high-energy nuclear collisions. *J. Phys. G* **2009**, *36*, 064022. [CrossRef]
42. van Hecke, H.; Sorge, H.; Xu, N. Evidence of early multi-strange hadron freeze-out in high energy nuclear collisions. *Phys. Rev. Lett.* **1998**, *81*, 5764–5767. [CrossRef]

43. Shor, A. ϕ-Meson Production as a probe of the quark–qluon plasma. *Phys. Rev. Lett.* **1985**, *54*, 1122–1125. [CrossRef]
44. Ishikawa, T.; Ahn, D.S.; Ahn, J.K.; Akimune, H.; Chang, W.C.; Daté, S.; Fujimura, H.; Fujiwara, M.; Hicks, K.; Hotta, T.; et al. ϕ photo-production from Li, C, Al, and Cu nuclei at E_γ = 1.5–2.4 GeV. *Phys. Lett. B* **2005**, *608*, 215. [CrossRef]
45. Alt., C. et al. [NA49 Collaboration]. Energy dependence of ϕ meson production in central Pb+Pb collisions at $\sqrt{s_{NN}}$ = 6 to 17 GeV. *Phys. Rev. C* **2008**, *78*, 044907. [CrossRef]
46. Abelev, B.I. et al. [STAR Collaboration]. Measurements of ϕ meson production in relativistic heavy-ion collisions at the BNL Relativistic Heavy Ion Collider (RHIC). *Phys. Rev. C* **2009**, *79*, 064903. [CrossRef]
47. Abelev, B. et al. [ALICE Collaboration]. $K^*(892)^0$ and ϕ (1020) production in Pb–Pb collisions at $\sqrt{s_{NN}}$ = 2.76 TeV. *Phys. Rev. C* **2015**, *91*, 024609. [CrossRef]
48. Acharya, S. et al. [ALICE Collaboration]. Production of $K^*(892)^0$ and ϕ (1020) in *pp* and Pb–Pb collisions at $\sqrt{s_{NN}}$ = 5.02 TeV. *Phys. Rev. C* **2022**, *106*, 034907. [CrossRef]
49. Feng, Y.-T.; Shao, F.-L.; Song, J. Averaged transverse momentum correlations of hadrons in relativistic heavy-ion collisions. *Phys. Rev. C* **2022**, *106*, 034910. [CrossRef]
50. Adam, J. et al. [ALICE Collaboration]. Centrality dependence of pion freeze-out radii in Pb–Pb collisions at $\sqrt{s_{NN}}$ = 2.76 TeV. *Phys. Rev. C* **2016**, *93*, 024905. [CrossRef]
51. Aamodt, K. et al. [ALICE Collaboration]. Two-pion Bose–Einstein correlations in central Pb–Pb collisions at $\sqrt{s_{\rm NN}}$ = 2.76 TeV. *Phys. Lett. B* **2011**, *696*, 328–337. [CrossRef]
52. Heinz, U.W. Concepts of heavy-ion physics. In *2003 CERN–CLAF School of High-Energy Physics*; Ellis., N., Ed.; CERN: Geneva, Switzerland, 2006; pp. 165–237. [CrossRef]
53. Abelev, B. et al. [STAR Collaboration]. Systematic measurements of identified particle spectra in *pp*, *d*+Au and Au+Au collisions ate the STAR detector. *Phys. Rev. C* **2009**, *79*, 034909. [CrossRef]
54. Abelev, B. et al. [ALICE Collaboration]. Centrality dependence of π, *K* and *p* production in Pb–Pb Collisions at $\sqrt{s_{NN}}$ = 2.76 TeV. *Phys. Rev. C* **2013**, *88*, 044910. [CrossRef]
55. Arnison, G. et al. [UA1 Collaboration]. Transverse momentum spectra for charged particles at the CERN proton–antiproton collider. *Phys. Lett. B* **1982**, *118*, 167–172. [CrossRef]
56. Adams, J.; Aggarwal, M.M.; Ahammed, Z.; Amonett, J.; Anderson, B.D.; Anderson, M.; Arkhipkin, D.; Averichev, G.S.; Bai, Y.; Barannikova, O.; et al. Multiplicity dependence of inclusive p_t spectra from $p-p$ collisions at $\sqrt{s}$ = 200 GeV. *Phys. Rev. D* **2006**, *74*, 032006. [CrossRef]
57. Aamodt, K. et al. [ALICE Collaboration]. Transverse momentum spectra of charged particles in proton–proton collisions at $\sqrt{s}$ = 900 GeV with ALICE at the LHC. *Phys. Lett. B* **2010**, *693*, 53–68. [CrossRef]
58. Skands, P.Z. Tuning Monte Carlo generators: The Perugia tunes. *Phys. Rev. D* **2010**, *82*, 074018. [CrossRef]
59. ALICE Collaboration. Multiplicity dependence of the average transverse momentum in pp, p–Pb, and Pb–Pb collisions at the LHC. *Phys. Lett. B* **2013**, *727*, 371–380. [CrossRef]
60. Adamczyk, L. et al. [STAR Collaboration]. Energy dependence of moments of net-proton multiplicity distributions at RHIC. *Phys. Rev. Lett.* **2014**, *112*, 032302. [CrossRef]
61. Adamczyk, L. et al. [STAR Collaboration]. Beam-energy dependence of the directed flow of protons, antiprotons, and pions in Au+Au collisions. *Phys. Rev. Lett.* **2014**, *112*, 162301. [CrossRef]
62. Adamczyk, L. et al. [STAR Collaboration]. Beam-energy dependence of directed flow of Λ, anti-Λ, $K^\pm$, K^0_S, and ϕ in Au + Au collisions. *Phys. Rev. Lett.* **2018**, *120*, 062301. [CrossRef] [PubMed]
63. Lin, Z.-W.; Ko, C.M.; Li, B.-A.; Zhang, B.; Pal, S. Multiphase transport model for relativistic heavy ion collisions. *Phys. Rev. C* **2005**, *72*, 064901. [CrossRef]
64. He, Y.; Lin, Z.W. Improved quark coalescence for a multi-phase transport model. *Phys. Rev. C* **2017**, *96*, 014910. [CrossRef]
65. Wang, X.N.; Gyulassy, M. HIJING: A Monte Carlo model for multiple jet production in *pp*, *p A*, and *A A* collisions. *Phys. Rev. D* **1991**, *44*, 3501–3516. [CrossRef]
66. Zhang, B. Comput. ZPC 1.0.1: A parton cascade for ultrarelativistic heavy ion collisions. *Phys. Commun.* **1998**, *109*, 193–206. [CrossRef]
67. Li, B.A.; Ko, C.M. Formation of superdense hadronic matter in high energy heavy-ion collisions. *Phys. Rev. C* **1995**, *52*, 2037–2063. [CrossRef] [PubMed]
68. Li, B.A.; Sustich, A.T.; Zhang, B.; Ko, C.M. Studies of superdense hadronic matter in A Relativistic Transport model. *Int. J. Mod. Phys. E* **2001**, *10*, 267–352. [CrossRef]

Disclaimer/Publisher's Note: The statements, opinions and data contained in all publications are solely those of the individual author(s) and contributor(s) and not of MDPI and/or the editor(s). MDPI and/or the editor(s) disclaim responsibility for any injury to people or property resulting from any ideas, methods, instructions or products referred to in the content.